PNAS
www.pnas.org

Supplementary Information for

Activity-dependent visualization and control of neural circuits for courtship behavior in the fly *Drosophila melanogaster*

Seika Takayanagi-Kiya, Taketoshi Kiya*

Taketoshi Kiya
Email: kiya@staff.kanazawa-u.ac.jp

This PDF file includes:

Supplementary text
Figs. S1 to S12
Table S1
Captions for movies S1 to S7
References for SI reference citations

Other supplementary materials for this manuscript include the following:

Movies S1 to S7

www.pnas.org/cgi/doi/10.1073/pnas.1814628116

Supplementary Text

Establishment and validation of *Hr38-GAL4* line

To establish methods to label neural circuits in an activity-dependent manner, we screened fly lines that have transgene insertion near the *Hr38* genomic locus and identified *P(PZ)Hr38[02306]*, a previously reported *Hr38-LacZ* enhancer trap line (1), as a neural activity reporter (Fig. S1A-D). In this line, the *LacZ* transgene is located immediate upstream of the transcription start site of *Hr38* (Fig. S1A). We first tested if the expression level of *LacZ* transcripts increases in response to light stimulation. *P(PZ)Hr38* flies were dark-adapted overnight, and then exposed to white light (15W, HITACHI) for 1 h. Transcript levels of *LacZ* and endogenous *Hr38* in the fly heads were quantified by qRT-PCR, and we detected increased expression of both genes in the light-stimulated group (Fig. S1B). Next, we examined if artificial neural activation can cause upregulation of *LacZ* expression in the brain. Here, we used flies carrying *P(PZ)Hr38* and expressing dTrpA1 in the mushroom body neurons under the control of *OK107-GAL4*, and confirmed neural activity-dependent increase in the levels of *LacZ* and *Hr38* transcripts (Fig. S1C). Further, when *P(PZ)Hr38* flies which pan-neuronally express dTrpA1 were thermogenetically stimulated, βGAL protein was detected by immunohistochemistry in the central area of the brain (Fig. S1D). The staining pattern was similar to the expression pattern of *Hr38* mRNA in pan-neuronally activated flies revealed by *in situ* hybridization in our previous study (2). Collectively, these results indicate that *LacZ* expression in *P(PZ)Hr38* line reflects expression of endogenous *Hr38*.

To expand the utility of this line by applying it to the GAL4/UAS system, we generated a *Hr38-GAL4* line by *P*-element-mediated genetic conversion (3). We confirmed that *LacZ* is precisely replaced with *GAL4* by DNA sequencing. In *Hr38-GAL4* flies, light-stimulation upregulated expression of *GAL4* mRNA in a similar manner to that of *Hr38* (Fig. S1E), indicating that *GAL4* is expressed in a neural activity-dependent manner. Next, we examined if the *Hr38-GAL4* line is useful for activity-dependent labeling of neural circuits by crossing it to a *UAS-*

mCD8GFP line, which expresses plasma membrane-targeted GFP under the control of GAL4. Since *Hr38* is expressed in the brain of naïve male fly in response to rearing with a virgin female (2), we first investigated whether the expression pattern of GFP resembles that of *Hr38* mRNA when males are reared with a female (Fig. S1F). However, many GFP-positive cells were detected in the brain of a naïve fly singly housed from eclosion and we were not able to clearly identify female-responsive cells. Thus, to prevent background GFP expression that may have occurred during development, we exploited the *tub-GAL80^{ts}* line, which ubiquitously expresses a temperature-sensitive form of GAL4 repressor (4). By temporally restricting GAL4 activity only to the stimulation period (Fig. S1G), we confirmed that *Hr38-GAL4* line is useful for labeling neurons activated by rearing with a virgin female (Fig. 1).

In the present study, we established a *Hr38-GAL4* line using the *P{IT.GAL4}* cassette, which allows conversion of the *GAL4* to *LexA*, *QF*, or a desired transgene through the InSITE (Integrase Swappable *In Vivo* Targeting Element) system (5). To expand the utility of *Hr38*-dependent transgene expression, we generated *Hr38-LexA*, *Hr38-QF*, and *Hr38-luciferase* lines by genetic swap or plasmid injection. However, these lines did not show activity-dependent reporter expression and were not useful, probably because changes and addition of sequences in the promoter region which inevitably accompany the genetic swap disturbed precise expression patterns of transgenes in our cases. Thus, in future studies, it will be important to knock-in a reporter cassette to the *Hr38* promoter region with minimal sequence addition, or use the HACK (Homology Assisted CRISPR Knock-in) method (6) or the 2A peptide-mediated system, to generate lines that utilize other genetic effectors.

qRT-PCR

Total RNA was isolated from 10 heads for each sample using RNAiso plus (Takara-Bio, Otsu, Japan), and three or four samples were analysed for each data point. The total RNA was treated with DNase I (Promega) and reverse-transcribed with PrimeScript RT reagent kit (Takara-Bio),

according to the manufacturer's protocol. Real-time RT-PCR was performed with *Premix Ex Taq*™ (Probe qPCR) (*Drpl3*, *Dhr38*, *GAL4*) or *Premix Ex Taq*™ II (Tli RNaseH Plus) (*LacZ*) (Takara-Bio), using gene-specific primers [*Drosophila rpl3* (*Drpl3*); 5'-AAGAAGCGCTCAGCTCGCCA-3' and 5'-ATGCCGGCCTTGTAGCCGAT-3', *Dhr38*; 5'-ATTCGGCGGCAAGTTCGCCA-3' and 5'-TGTCGCCACAAACGGCACACA-3', *GAL4*; 5'-TCGCATCGCTCAGTCACGCCTT-3' and 5'-AAAGCAGACGGGGTCAGTGGCA-3', *LacZ*; 5'-TGCCGCCTGTTTTGACCGCT-3' and 5'-TTCAATTCGCGCGTCCCGCA-3'] and gene-specific Taqman probes [*Drpl3*; 5'-FAM-CCCCAAGGATGACGCCAGCAAGCCA-BHQ-3', *Dhr38*; 5'-FAM-CCGTTTGCTCCAGGCTCCGTCGCAG-BHQ-3', *GAL4*; 5'-FAM-AGGGCAACAGCAACAGCTGCAATCA-BHQ-3']. The fluorescent signals from samples were obtained using ABI7900HT (Applied Biosystems, Foster City, CA) with default settings. PCR products amplified by each set of primers were purified using a PCR purification kit (Qiagen), serially diluted (10-fold dilutions for a dynamic range of 10^6), and used as quantification standards. The determined value of each sample was normalized by that of *Drpl3*. The normalized values were again normalized to the mean value of control samples, and shown as the relative expression. All data are presented as mean ± standard error.

Activation of *OK371^{fru}* neurons by dTrpA1

Male flies were raised at 23˚C, collected within a few hours after eclosion and single-reared at 23˚C until experiments (5-10 days). Males of the experimental group were transferred to behavior recording box pre-warmed to 31˚C and their courtship behavior to a CS virgin female (3-5 day-old) was video-recorded for 20 min. Control males were assayed in 23˚C. Antennae ablation was conducted immediately after eclosion.

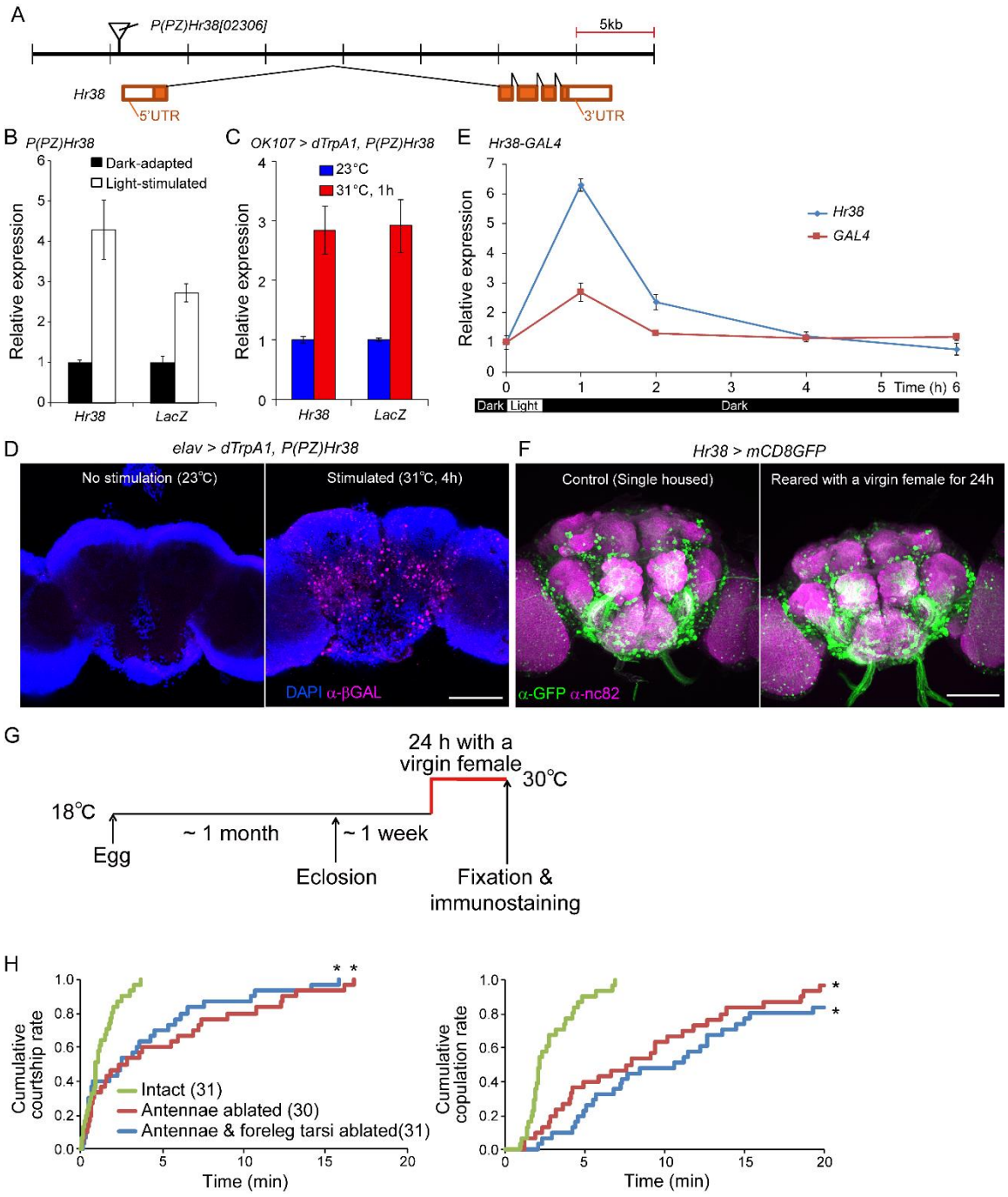

Fig. S1. Establishment of *Hr38-GAL4* line and schematics of the experiments.

(A) The genomic structure of *Hr38* gene and the site of *P(PZ)* (*LacZ* transgene) insertion. (B, C) Levels of *Hr38* and *LacZ* transcripts in the heads of *P(PZ)Hr38* flies in response to light-stimulation (B) or thermogenetic activation of the mushroom body neurons (C) revealed by qRT-PCR. N = 3, each. (D) Pictures of anti-βGAL and DNA (DAPI) staining of the brains.

Thermogenetic pan-neuronal activation was induced (right panel) in flies that possess *P(PZ)Hr38* insertion. Scale bar: 100μm. (E) Time-course of *Hr38* and *GAL4* expression revealed by qRT-PCR. Flies of *Hr38-GAL4* line dark-adapted overnight were stimulated with white light for 30 min. N = 4, each. (F) GFP expression pattern of *Hr38>mCD8GFP* strain (without *tub-GAL80^{ts}*) reared with (right) or without (left) a virgin female. Each male was singly housed in a small glass vial from eclosion. Scale bar: 100μm. (G) A schematic of temperature-shift protocol using *tub-GAL80^{ts}*, presented in Fig. 1-3, S1H, S2-10. Flies were reared at 18˚C, under which ubiquitously expressed GAL80^{ts} inhibits GAL4 activity, until subjected to experiment. Isolated adult male flies were moved to 30˚C to inactivate GAL80^{ts} and allow transgene expression. (H) Cumulative rate of male flies that courted (left) or copulated (right) plotted against time. Antennae removal significantly inhibited courtship initiation and copulation performance (*: $P < 0.05$, Log-rank test. Compared with intact flies), but further ablation of foreleg tarsi had no significant effects. Antennae and foreleg tarsi were surgically removed under CO_2 anesthetization immediately after eclosion. Experiments were conducted at 30˚C using flies raised and kept at 18˚C until experiment.

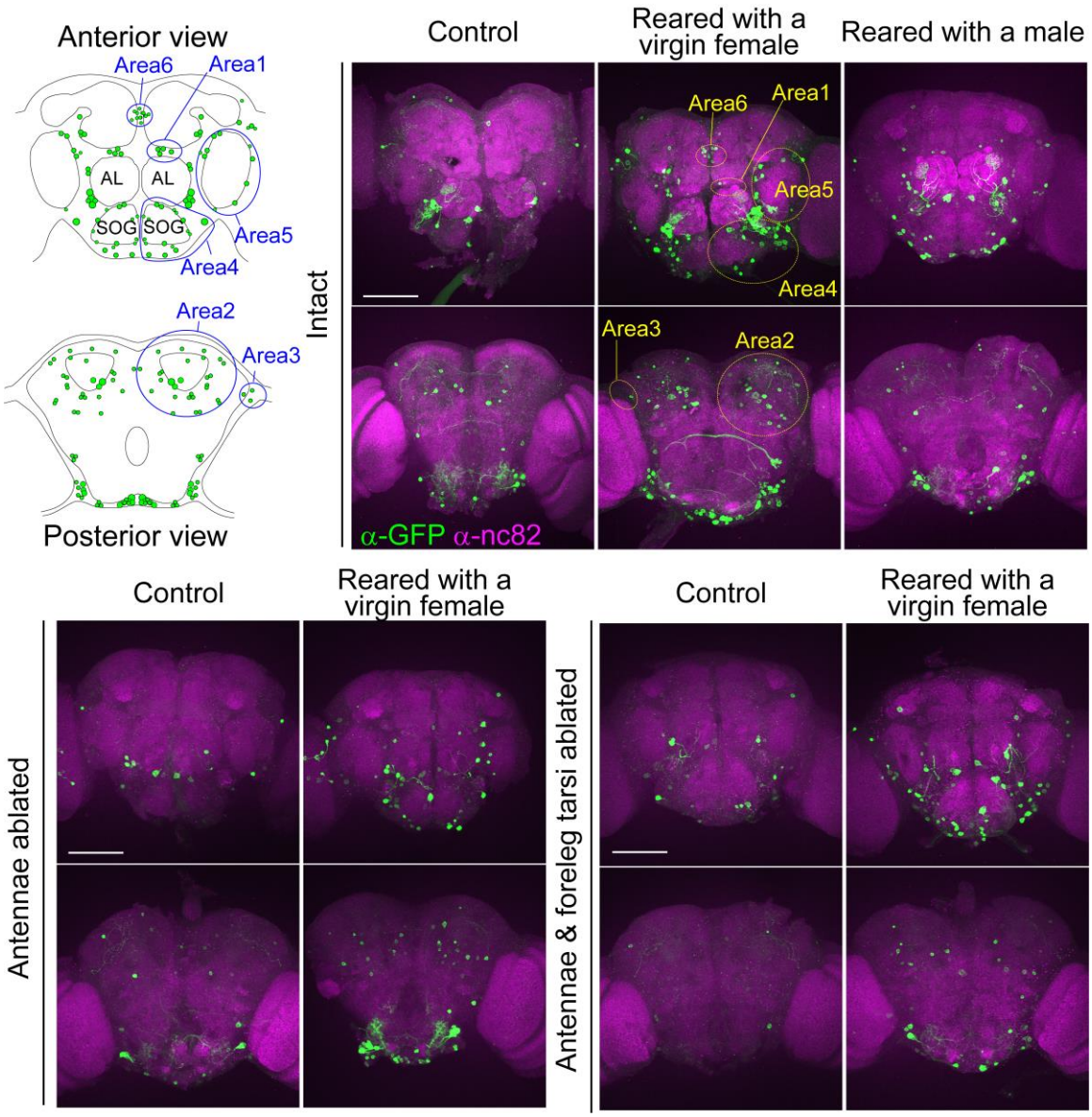

Fig. S2. High magnification pictures of the brain in *Hr38>mCD8GFP* males.

Anti-GFP and anti-nc82 staining of intact, antennae-ablated, and antennae- and foreleg tarsi-ablated males. Scale bars: 100μm.

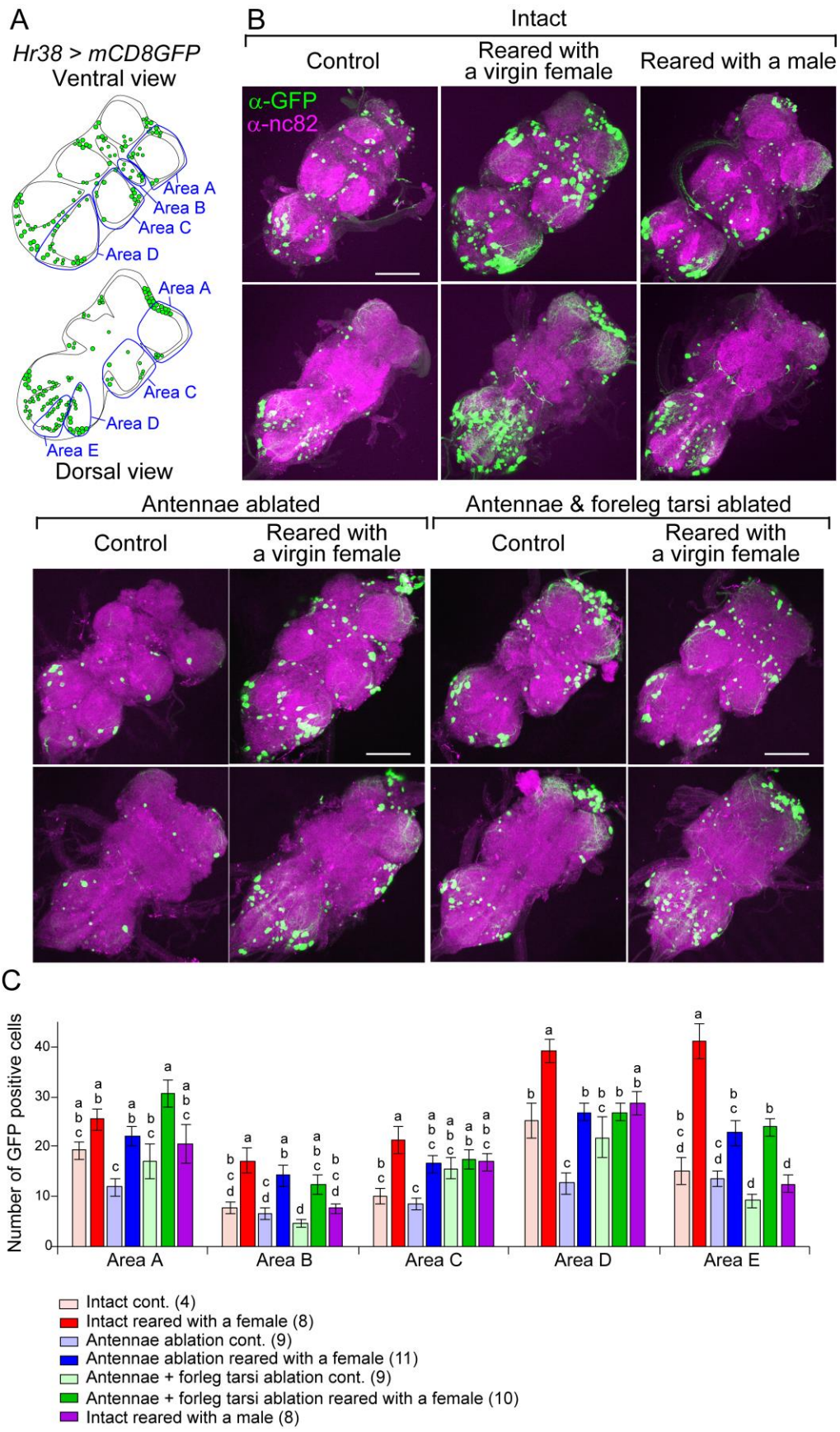
A
Hr38 > mCD8GFP
Ventral view
Area A
Area B
Area C
Area D
Area A
Area C
Area D
Area E
Dorsal view
B
Intact
Control
Reared with a virgin female
Reared with a male
α-GFP
α-nc82
Antennae ablated
Antennae & foreleg tarsi ablated
Control
Reared with a virgin female
Control
Reared with a virgin female
C
Number of GFP positive cells
0
10
20
30
40
Area A
Area B
Area C
Area D
Area E
Intact cont. (4)
Intact reared with a female (8)
Antennae ablation cont. (9)
Antennae ablation reared with a female (11)
Antennae + forleg tarsi ablation cont. (9)
Antennae + forleg tarsi ablation reared with a female (10)
Intact reared with a male (8)

Fig. S3. Activity-dependent labeling of VNC neural circuits in response to rearing with a female or a male.

(A) Schematics of GFP expression pattern in the VNC of intact males reared with a virgin female. (B) Pictures of anti-GFP immunostaining of the male VNCs under different conditions. Scale bars: 100μm. (C) Number of GFP-positive cells in each area under different conditions. Statistically different groups are indicated by different alphabets ($P < 0.05$, Tukey-Kramer's HSD test after ANOVA).

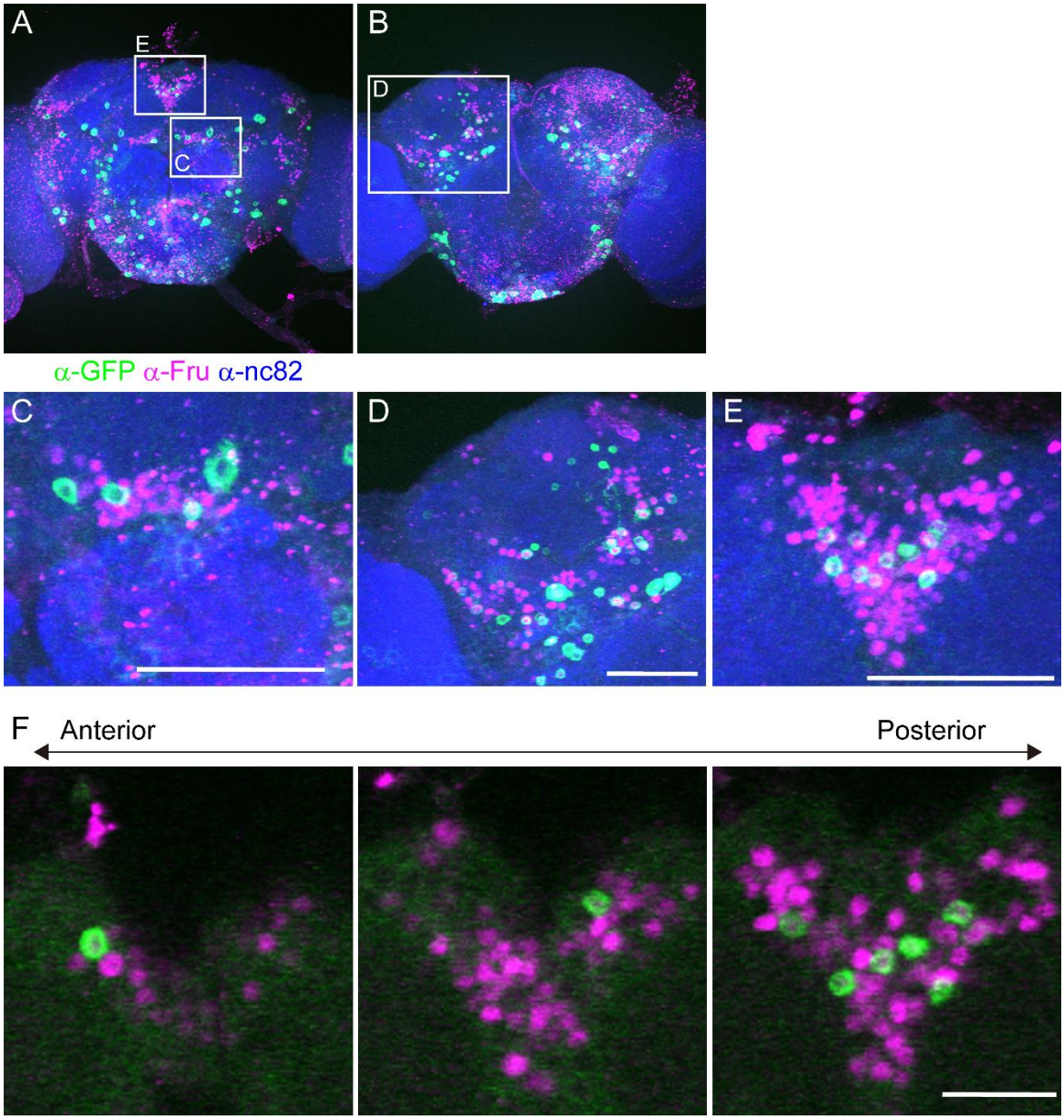

Fig. S4. Colocalization analysis of activity-dependently GFP-labeled cells and Fruitless in the brain of male reared with a female.

(A, B) Pictures of anti-GFP (green), anti-Fruitless (magenta), and anti-nc82 (blue) staining of the brain of a male reared with a virgin female. Anterior (A) and posterior (B) views. (C-E) High magnification pictures corresponding to area 1, 2, and 6, respectively. Scale bars: 50μm. (F) Pictures of single optical planes in (E). Scale bar: 20μm.

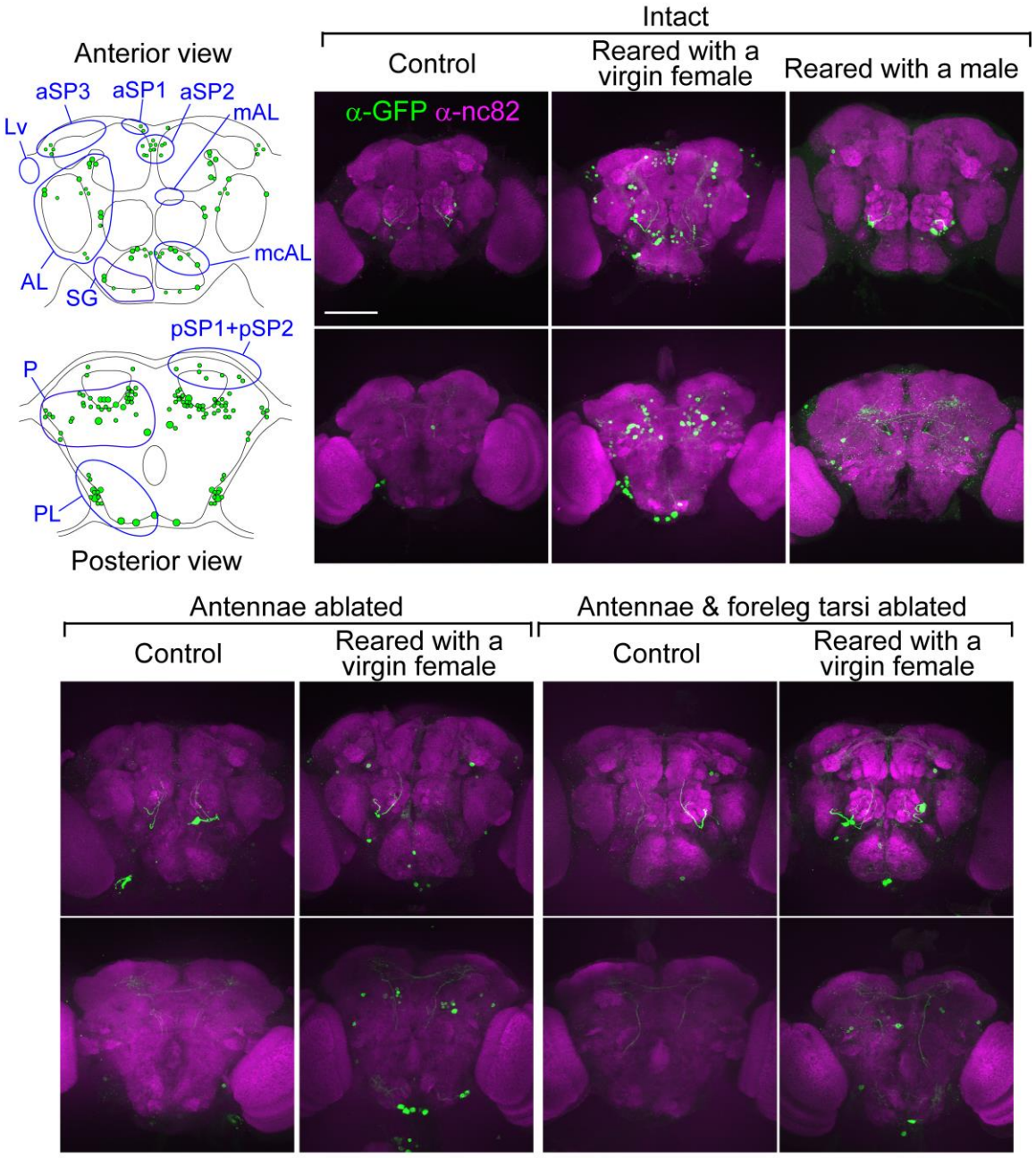

Fig. S5. High magnification brain pictures of males with *fru*-restricted labeling.

Anti-GFP and anti-nc82 staining of the brains of intact, antennae-ablated, and antennae- and foreleg tarsi-ablated males. Scale bar: 100μm.

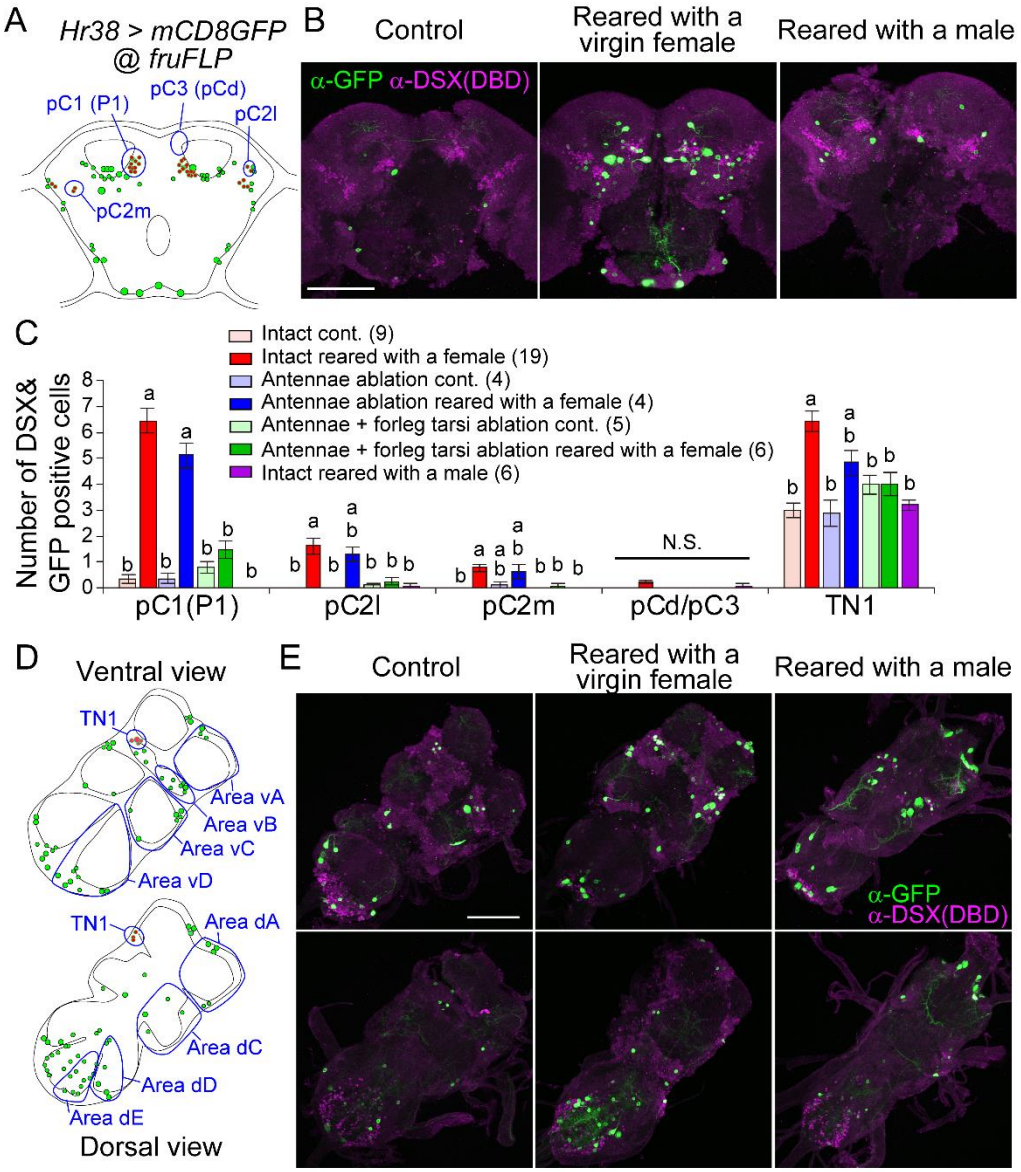
A
Hr38 > mCD8GFP
@ fruFLP
pC1 (P1)
pC3 (pCd)
pC2l
pC2m
B
Control
Reared with a virgin female
Reared with a male
α-GFP α-DSX(DBD)
C
Intact cont. (9)
Intact reared with a female (19)
Antennae ablation cont. (4)
Antennae ablation reared with a female (4)
Antennae + forleg tarsi ablation cont. (5)
Antennae + forleg tarsi ablation reared with a female (6)
Intact reared with a male (6)
Number of DSX& GFP positive cells
N.S.
pC1(P1)
pC2l
pC2m
pCd/pC3
TN1
D
Ventral view
TN1
Area vA
Area vB
Area vC
Area vD
TN1
Area dA
Area dC
Area dD
Area dE
Dorsal view
E
Control
Reared with a virgin female
Reared with a male
α-GFP
α-DSX(DBD)
F
Number of GFP positive cells
Area vA
Area vB
Area vC
Area vD
Intact cont. (8)
Intact reared with a female (16)
Antennae ablation cont. (10)
Antennae ablation reared with a female (9)
Antennae + forleg tarsi ablation cont. (8)
Antennae + forleg tarsi ablation reared with a female (10)
Intact reared with a male (11)
Area dA
Area dC
Area dD
Area dE

Fig. S6. Detailed GFP expression analysis in the brains and VNCs of males with *fru*-restricted labeling.

(A, D) Schematics of GFP expression pattern in the brain and VNC of intact male reared with a virgin female. (B, E) Pictures of anti-GFP and anti-Doublesex immunostaining of the male brains and VNCs under different conditions. Scale bars: 100μm. (C, F) Number of GFP positive cells in each neural cluster or area under different conditions. Only cells double-positive to GFP and DSX were counted in the brain or TN1 of the VNC (C). Statistically different groups are indicated by different alphabets ($P < 0.05$, Tukey-Kramer's HSD test after ANOVA).

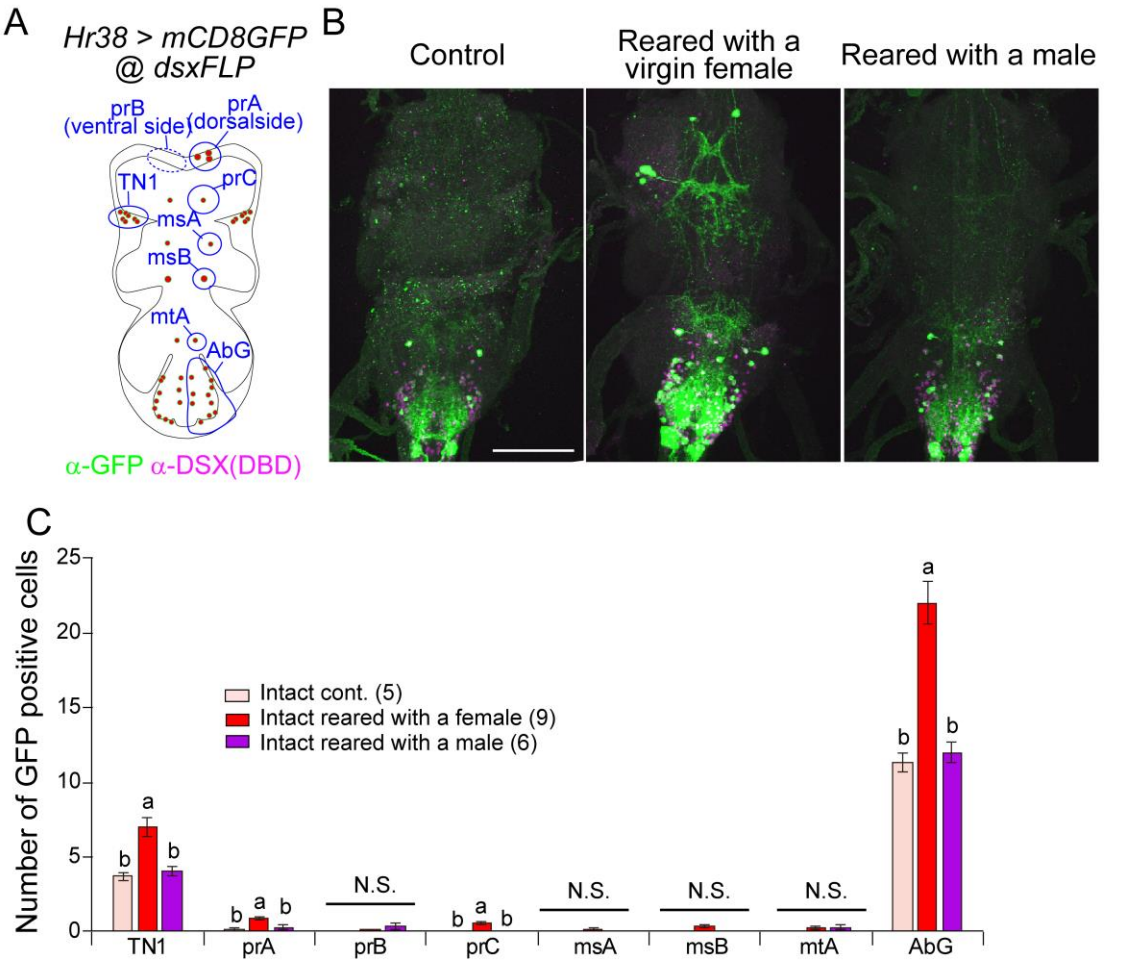

Fig. S7. Activity-dependent labeling of VNC neural circuits in males with *dsx*-restricted labeling.

(A) Schematics of GFP expression pattern in the VNC of intact males reared with a virgin female. (B) Pictures of anti-GFP and anti-Doublesex immunostaining of the male VNCs under different conditions. Scale bar: 100μm. (C) Number of GFP-positive cells in each neural cluster under different conditions. Statistically different groups are indicated by different alphabets ($P < 0.05$, Tukey-Kramer's HSD test after ANOVA).

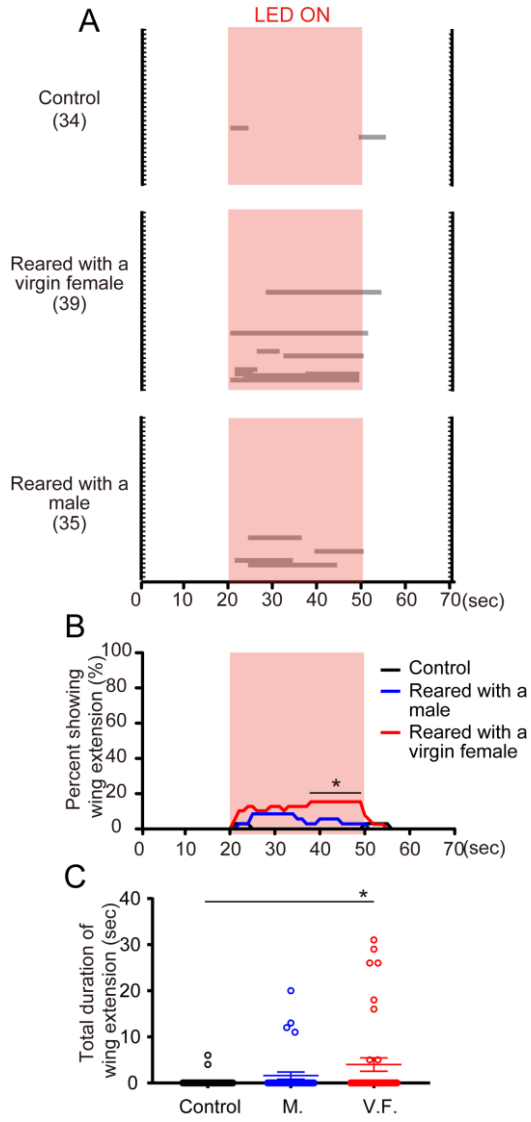

Fig. S8. Induction of wing extension by reactivation of *fru* neurons activity-dependently labeled by rearing with a female.

(A) Raster plots of wing extension in response to red light. Red shades indicate exposure to red light. (B) Rates of animals exhibiting wing extension, based on (A). *: $P < 0.05$, *Fisher*'s exact test performed for each second. The black line indicates the time range where significant difference was observed between control and males reared with a virgin female. (C) Total duration of wing extension during the observation period. M.: reared with a male, V.F.: reared with a virgin female. *: $P < 0.05$, Mann-Whitney *U*-test.

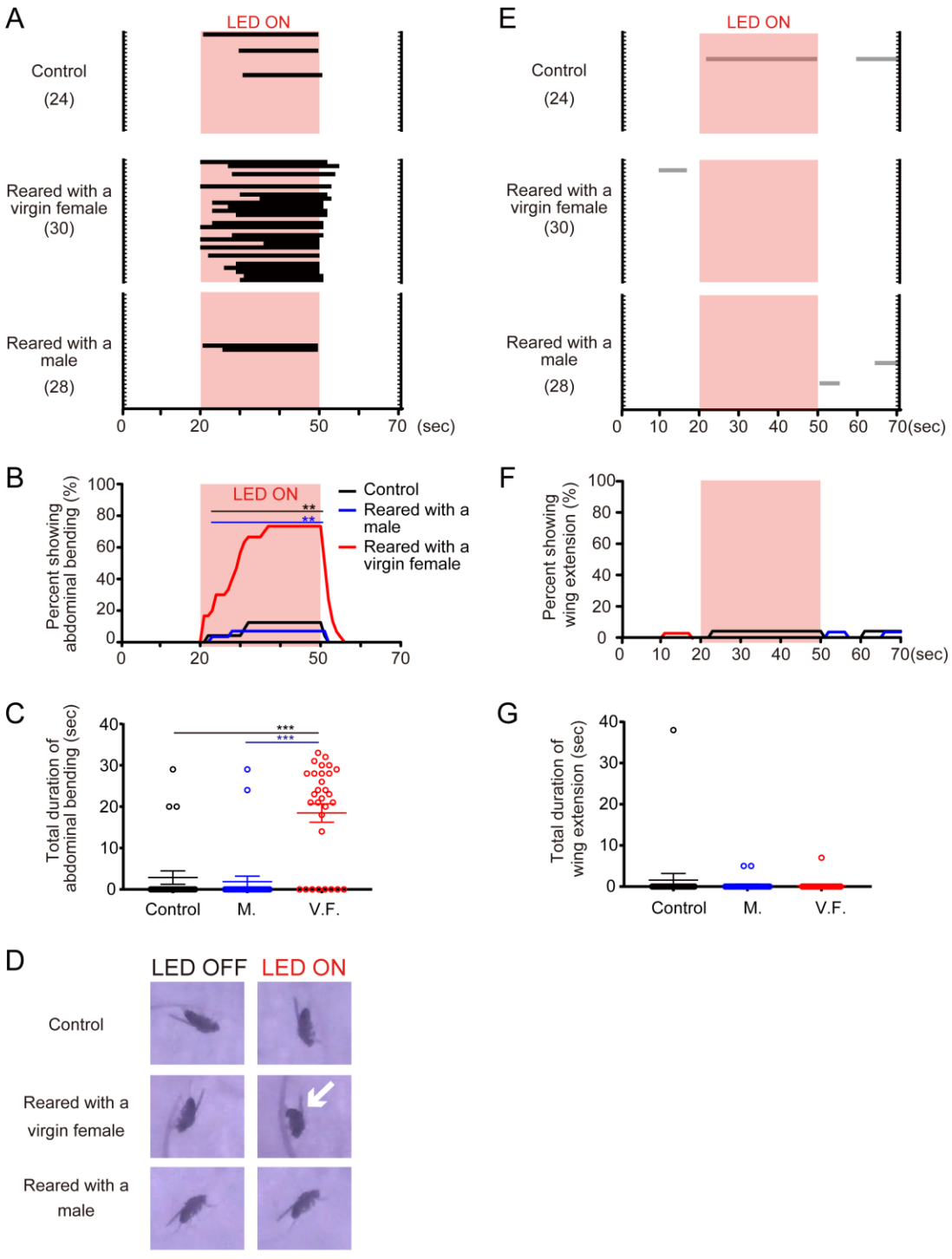

Fig. S9. Optogenetic reactivation of *dsx* neurons activity-dependently labeled by previous experience.

(A, E) Raster plots showing the occurrence of abdominal bending (A) or wing extension (E) in response to red light. Red shades indicate light exposure (30 sec). (B, F) Percentage of flies showing abdominal bending (B) or wing extension (F), based on (A, E). **: $P < 0.01$, *Fisher*'s exact test performed for each second. Black and blue lines indicate the time range where significant differences were observed when males reared with a virgin female were compared to control, and to males reared with a male, respectively. (C, G) Total duration of abdominal bending (C) or wing extension (G) during the observation period. M.: reared with a male, V.F.: reared with a virgin female. ***: $P < 0.001$, Mann-Whitney *U*-test. (D) Representative images taken from supplementary movies (Movies S5-S7). White arrow indicates the fly showing abdominal bending.

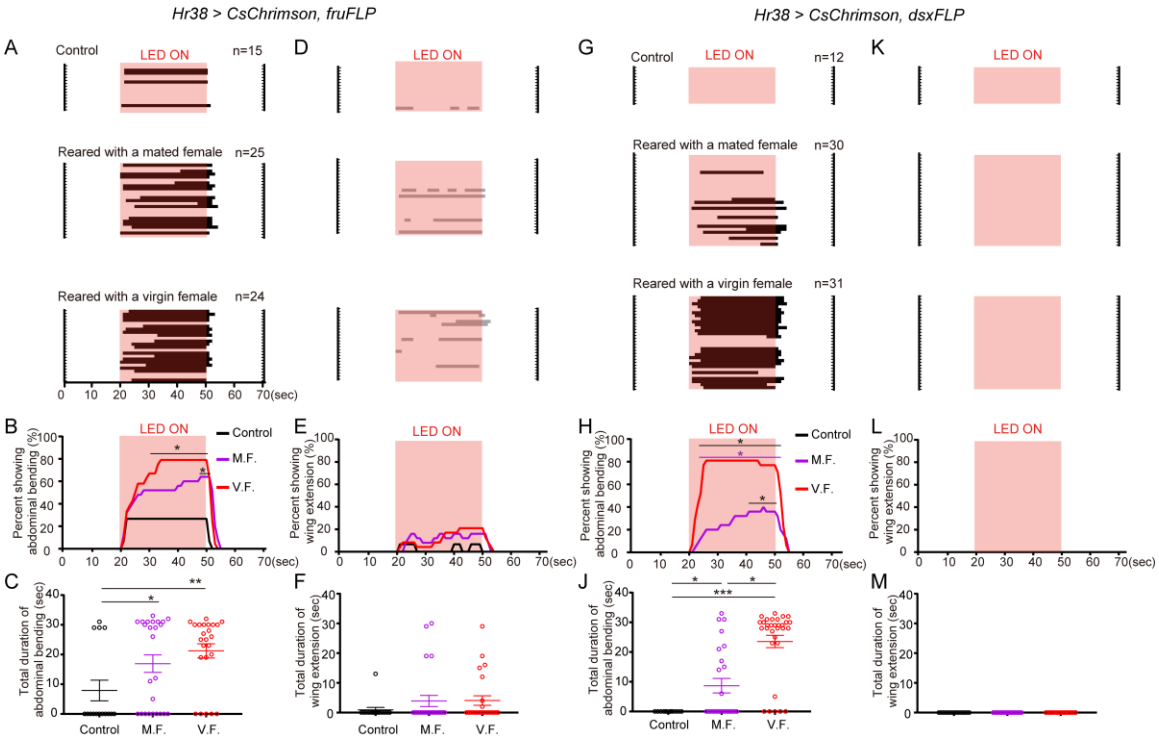

Fig. S10. Optogenetic reactivation of *fru* or *dsx* neurons labeled by rearing with a virgin or mated female.

(A, D, G, K) Raster plots showing the occurrence of abdominal bending (A, G) or wing extension (D, K) in response to red light (627nm LED, 9.9 and 84.6 μW/mm^2 for *fru*- and *dsx*-restricted, respectively). Red shades indicate light exposure (30 sec). (B, E, H, L) Percentage of flies showing abdominal bending (B, H) or wing extension (E, L). *: $P < 0.05$, *Fisher*'s exact test performed for each second. Black and purple lines indicate the time range where significant differences were observed compared with control and males reared with a mated female, respectively. (C, F, J, M) Total duration of abdominal bending (C, J) or wing extension (F, M) during the observation period. M.F.: reared with a mated female, V.F.: reared with a virgin female. *: $P < 0.05$, **: $P < 0.01$, ***: $P < 0.001$, Mann-Whitney *U*-test.

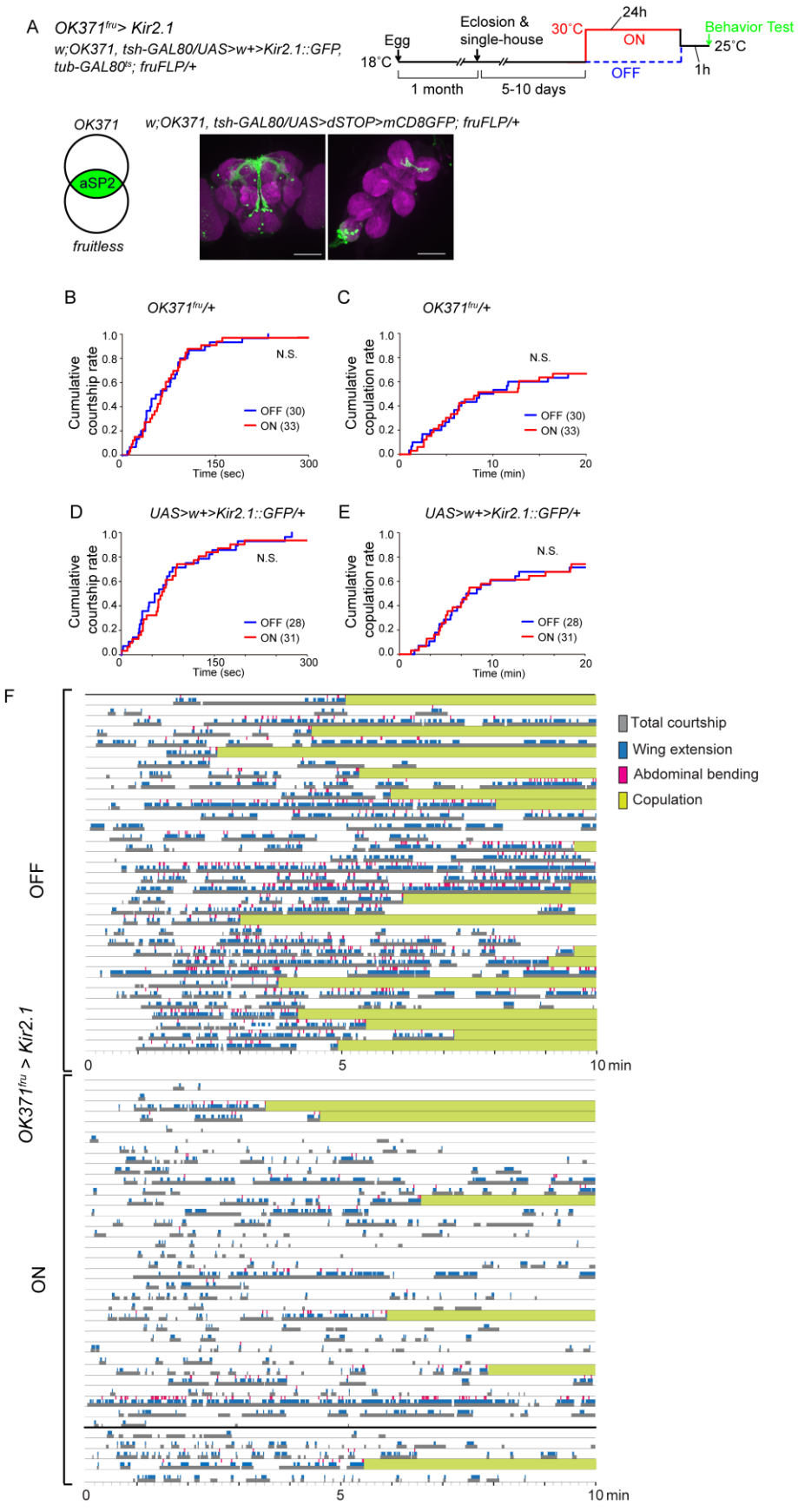
A
OK371fru> Kir2.1
w;OK371, tsh-GAL80/UAS>w+>Kir2.1::GFP,
tub-GAL80ts; fruFLP/+
Egg
18°C
Eclosion &
single-house
1 month
5-10 days
30°C
24h
ON
OFF
1h
Behavior Test
25°C
OK371
aSP2
fruitless
w;OK371, tsh-GAL80/UAS>dSTOP>mCD8GFP; fruFLP/+
B
OK371fru/+
Cumulative courtship rate
N.S.
OFF (30)
ON (33)
Time (sec)
C
OK371fru/+
Cumulative copulation rate
N.S.
OFF (30)
ON (33)
Time (min)
D
UAS>w+>Kir2.1::GFP/+
Cumulative courtship rate
N.S.
OFF (28)
ON (31)
Time (sec)
E
UAS>w+>Kir2.1::GFP/+
Cumulative copulation rate
N.S.
OFF (28)
ON (31)
Time (min)
F
OFF
ON
OK371fru > Kir2.1
Total courtship
Wing extension
Abdominal bending
Copulation
0
5
10 min

Fig. S11. Behavioral analyses of *OK371^{fru}>Kir2.1* flies.

(A) Upper panels: The genotype of flies (left) and time-course of the temperature-shift experiment (right) in Fig. 4. *>w+>* indicates FRT-flanked *mini-white* gene and stop cassette. Lower panels: A schematic drawing of intersectional approach to achieve transgene expression in neurons including aSP2 neurons (left). Pictures of anti-GFP (green) and anti-nc82 (magenta) staining of the male brain and VNC of *OK371^{fru}>mCD8GFP* strain. In addition to aSP2 neurons, a small number of neurons showed GFP expression in the brain and abdominal ganglion. There were also GFP-positive neurites, possibly from the foreleg sensory organ. Scale bars: 100μm. (B-E) Cumulative courtship rate (B, D) and cumulative copulation rate (C, E) of male flies carrying *OK371^{fru}* driver or *UAS>w+>Kir2.1::GFP*. (F) Raster plots of courtship behaviors observed during the first 10 min in control (upper panel) and experimental (lower panel) males.

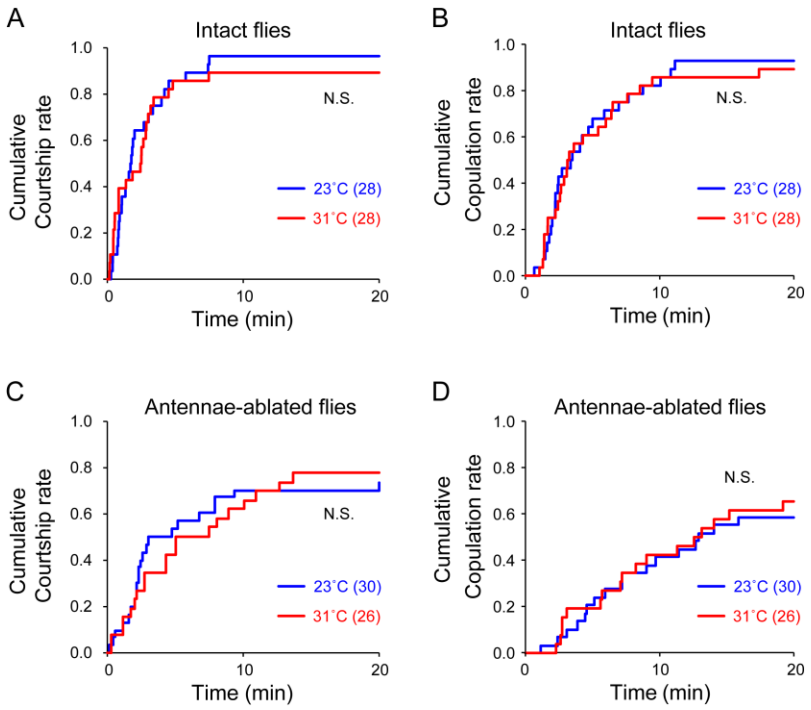

Fig. S12. Activation of *OK371^{fru}* neurons does not affect courtship or copulation latency.

Cumulative courtship (A, C) and copulation (B, D) rate of animals expressing dTrpA1 in *OK371^{fru}* neurons. Flies were raised and kept at 23˚C until experiment. Thermogenetic activation of *OK371^{fru}* did not affect courtship or copulation latency of intact (A, B) and antennae-ablated (C, D) male flies.

Table S1. Complete genotypes of flies used in this study

Relevant figures	Name	Genotype of flies used for the expreiment	Note
	P{IT.GAL4}	P{w[+mC]=IT.GAL4}A134.3, w[*]/FM6	GAL4 donor (Bloomington 33598)
	Canton-S	Wild type	
	white-eyed Canton-S	w/Y (2022U)	Gift from Takaomi Sakai
Figure 1, S1H, S2, S3, S4	Hr38>mCD8::GFP	w, tub-GAL80[ts]/Y; Hr38-GAL4, tub-GAL80[ts]/+; UAS-mCD8::GFP/+	
Figure S1A, B	P(PZ)Hr38 (Hr38-LacZ)	P{ry[+7.2]=PZ}Hr38[02306] cn[1]/CyO; ry[506]	Bloomington 11181
Figure S1C	OK107>dTrpA1, P(PZ)Hr38	yw, P(PZ)Hr38, UAS-dTrpA1/+;;OK107-GAL4/+	
Figure S1D	elav>dTrpA1, P(PZ)Hr38	elav-GAL4/+; P(PZ)Hr38, UAS-dTrpA1/+	
Figure S1E	Hr38-GAL4	w; Hr38-GAL4/CyO	Established in this study.
Figure S1F	Hr38>mCD8::GFP (without tub-GAL80[ts])	w/Y; Hr38-GAL4/+; UAS-mCD8::GFP/+	
Figure 2A-D, S5, S6	Hr38>mCD8::GFP (restricted to *fru*+ neurons)	w, tub-GAL80[ts]/Y; Hr38-GAL4, tub-GAL80[ts]/+; UAS>dSTOP>mCD8GFP/fruFLP	w; fruFLP/TM3: Gift From Barry Dickson
Figure 2E-G, S7	Hr38>mCD8::GFP (restricted to *dsx*+ neurons)	w/Y; Hr38-GAL4, tub-GAL80[ts]/+; UAS>dSTOP>mCD8GFP/dsxFLP	w; dsxFLP/TM3: Gift From Stephen Goodwin
Figure 3, S8, S10A-F	Hr38>CsChrimson (restricted to *fru*+ neurons)	w/Y; Hr38-GAL4, tub-GAL80[ts]/+; UAS>dsFRT>CsChrimson::mVenus/fruFLP	w; UAS>dsFRT>CsChrimson::mVenus/TM3: Gift From Gerry Rubin
Figure S9, S10G-M	Hr38>CsChrimson (restricted to *dsx*+ neurons)	w/Y; Hr38-GAL4, tub-GAL80[ts]/+; UAS>dsFRT>CsChrimson::mVenus/dsxFLP	
Figure 4, S11F	OK371^{fru}>Kir2.1	w/Y;OK371, tsh-GAL80/UAS>w+>Kir2.1::GFP, tub-GAL80[ts]; fruFLP/+	yw; tsh-GAL80/CyO: Gift from Julie Simpson w; UAS>stop>Kir2.1:GFP: Gift from Kenta Asahina
Figure S11B, C	OK371^{fru}/+	w/Y; OK371, tsh-GAL80/+; fruFLP/+	
Figure S11D, E	UAS-Kir2.1/+	w/Y; UAS>w+>Kir2.1::GFP, tub-GAL80[ts]/+	
Figure S12	OK371^{fru}>dTrpA1[mCherry]	w/Y; OK371/UAS>STOP>dTrpA1[mCherry]; fruFLP/+	w; UAS>STOP>dTrpA1[mCherry]/CyO: Gift from Anne von Philipsborn

Movie S1. Representative video of a control male exposed to red light (*Hr38>CsChrimson, fruFLP*). A white circle is shown when LED is on.

Movie S2. Representative video of a male reared with a virgin female exposed to red light (*Hr38>CsChrimson, fruFLP*). The fly exhibits abdominal bending. A white circle is shown when LED is on.

Movie S3. Representative video of a male reared with a male exposed to red light (*Hr38>CsChrimson, fruFLP*). A white circle is shown when LED is on.

Movie S4. Representative video of a male reared with a virgin female exposed to red light (*Hr38>CsChrimson, fruFLP*). The fly exhibits unilateral wing extension. A white circle is shown when LED is on.

Movie S5. Representative video of a control male exposed to red light (*Hr38>CsChrimson, dsxFLP*). A white circle is shown when LED is on.

Movie S6. Representative video of a male reared with a virgin female exposed to red light (*Hr38>CsChrimson, dsxFLP*). The fly exhibits abdominal bending. A white circle is shown when LED is on.

Movie S7. Representative video of a male reared with a male exposed to red light (*Hr38>CsChrimson, dsxFLP*). A white circle is shown when LED is on.

References

1. Kozlova T, *et al.* (1998) *Drosophila* hormone receptor 38 functions in metamorphosis: a role in adult cuticle formation. *Genetics* 149(3):1465-1475.

2. Fujita N, *et al.* (2013) Visualization of neural activity in insect brains using a conserved immediate early gene, Hr38. *Curr Biol* 23(20):2063-2070.
3. Sepp KJ & Auld VJ (1999) Conversion of lacZ enhancer trap lines to GAL4 lines using targeted transposition in Drosophila melanogaster. *Genetics* 151(3):1093-1101.
4. McGuire SE (2003) Spatiotemporal Rescue of Memory Dysfunction in Drosophila. *Science* 302(5651):1765-1768.
5. Gohl DM, *et al.* (2011) A versatile in vivo system for directed dissection of gene expression patterns. *Nature Methods* 8(3):231-237.
6. Lin CC & Potter CJ (2016) Editing Transgenic DNA Components by Inducible Gene Replacement in Drosophila melanogaster. *Genetics* 203(4):1613-1628.